



LAWRENCE  
LIVERMORE  
NATIONAL  
LABORATORY

# Dependence of the LH power threshold on the X-point radius

D. Battaglia, C. Chang, S. M. Kaye, S. Ku, R. Maingi, J. Ahn, R. E. Bell, A. Diallo, S. Gerhardt, B. P. LeBlanc, J. Menard, V. Soukhanovskii

June 23, 2011

38th European Physical Society Conference on Plasma Physics  
Strasbourg, France  
June 27, 2011 through July 1, 2011

## **Disclaimer**

---

This document was prepared as an account of work sponsored by an agency of the United States government. Neither the United States government nor Lawrence Livermore National Security, LLC, nor any of their employees makes any warranty, expressed or implied, or assumes any legal liability or responsibility for the accuracy, completeness, or usefulness of any information, apparatus, product, or process disclosed, or represents that its use would not infringe privately owned rights. Reference herein to any specific commercial product, process, or service by trade name, trademark, manufacturer, or otherwise does not necessarily constitute or imply its endorsement, recommendation, or favoring by the United States government or Lawrence Livermore National Security, LLC. The views and opinions of authors expressed herein do not necessarily state or reflect those of the United States government or Lawrence Livermore National Security, LLC, and shall not be used for advertising or product endorsement purposes.

## Dependence of the LH power threshold on the X-point radius

D.J. Battaglia<sup>1</sup>, C.-S. Chang<sup>2</sup>, S.M. Kaye<sup>2</sup>, S. Ku<sup>2,3</sup>, R. Maingi<sup>1</sup>, J.-W. Ahn<sup>1</sup>, R.E. Bell<sup>2</sup>,  
A. Diallo<sup>2</sup>, S. Gerhardt<sup>2</sup>, B.P. LeBlanc<sup>2</sup>, J. Menard<sup>2</sup>, V. Soukhanovskii<sup>4</sup>

<sup>1</sup> Oak Ridge National Laboratory, Oak Ridge, TN, USA

<sup>2</sup> Princeton Plasma Physics Laboratory, Princeton, NJ, USA

<sup>3</sup> New York University, New York City, NY, USA

<sup>4</sup> Lawrence Livermore National Laboratory, Livermore, CA, USA

Magnetically confined plasmas routinely undergo an abrupt (sub-ms) transition from low- to high-energy confinement (L-H transition) when a threshold in the plasma heating power ( $P_{\text{heat}} > P_{\text{LH}}$ ) is exceeded. Tokamak experiments, including the National Spherical Torus Experiment (NSTX), observe that  $P_{\text{LH}}$  varies with many of the experimental parameters that define the magnetic geometry, including the X-point radius ( $R_X$ ) [1]. This dependence is consistent with the X-transport theory, which describes the mean edge radial electric field ( $E_r$ ) profile, and thus the  $E_r \times B$  shearing rate, required to prevent non-ambipolar ion transport in a diverted tokamak plasma [2]. This paper presents the connection between the  $P_{\text{LH}}$  dependence on  $R_X$  in terms of the X-transport theory and provides experimental and modeling results from NSTX that are consistent with this theory.

The X-transport theory describes neoclassical orbits of collisionless ions near the plasma boundary with at least one X-point. The small poloidal magnetic field in the X-point region lengthens the poloidal transit time and the  $\nabla B$  drift of collisionless particles that pass through this region. The ion poloidal transit time through the X-point region is much longer than electrons, thus the enhanced  $\nabla B$  drift is non-ambipolar. The ions on orbits that leave the separatrix near the X-point are lost along open field lines to the divertor floor. Thus, a negative  $E_r$  just inside the plasma edge must develop to maintain quasi-neutrality.

The X-transport theory predicts the edge  $E_r$  profile is tightly coupled to both the magnetic geometry and the edge ion temperature ( $T_i$ ). The  $E_r$  profile within the plasma edge impacts the mean perpendicular flow and flow shear, which is presumed to play an important role in triggering the LH transition. Thus, the critical  $T_i$  for triggering the L-H transition will depend on the magnetic geometry of the plasma, including  $R_X$ . In other words,  $P_{\text{LH}}$  is predicted to vary with  $R_X$  presuming the edge  $T_i$  is coupled to the core plasma heating power.

A guiding center orbit calculation [3] is used to compute the collisionless ion orbits lost to the divertor in the absence of electric fields or flows in a single-null geometry with the

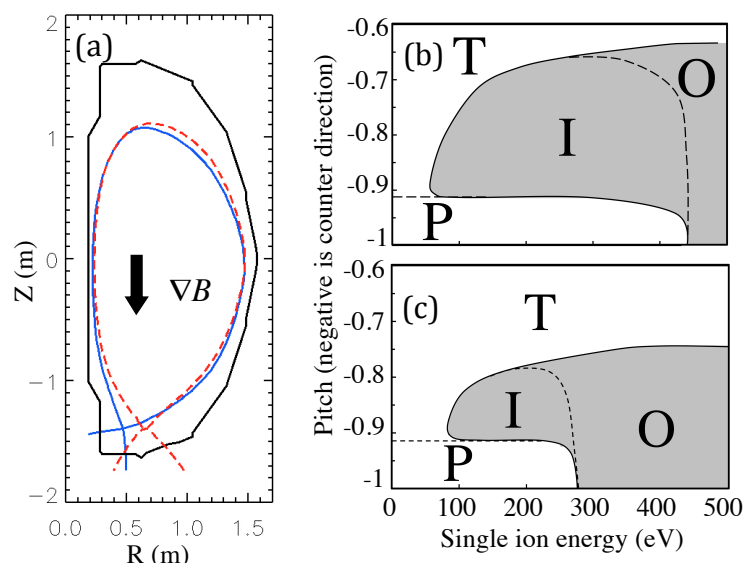


FIG 1 (a) Separatrix of small- $R_x$  shape (blue solid) and large- $R_x$  shape (red dashed), and ion loss hole calculations at  $\psi_N = 0.96$  on outboard midplane for the (b) large- $R_x$  and (c) small- $R_x$  shape.

ion  $\nabla B$  drift toward the single X-point. The calculations are completed for the two plasma shapes shown in Figure 1a. The velocity space loss hole in pitch-energy space for ions launched at  $\psi_N = 0.96$  at the outboard midplane are shown in Figures 1b-c. Ions launched with pitch and energy components in the unshaded region are either confined passing or trapped orbits (regions labeled P and T, respectively). The loss hole

(shaded region) is divided into the ions lost to the inner (I) and outer (O) divertor leg.

The loss hole for the large- $R_x$  shape has a lower critical energy (71 eV versus 95 eV) and is wider compared to the small- $R_x$  shape. The lower critical energy is due to (1) longer ion bounce orbits prior to entering the X-point region from the high-field side and (2) flux surfaces that are more “flat,” i.e., lower  $B_z$  in the X-point region. The loss cone is wider for the large- $R_x$  shape since more trapped orbits pass through the X-point region.

The percentage of collisionless ion orbits that originate at  $\psi_N = 0.96$  at the outboard midplane and are lost through the X-point is approximately equal for the two shapes if the Maxwellian ion temperature for the small- $R_x$  discharge is about 60% larger compared to the large- $R_x$  discharge. Therefore, the small- $R_x$  geometry will require a hotter edge ion temperature to achieve a similar number of ion loss orbits as the large- $R_x$  shape. A full self-consistent calculation of the  $E_r$  profile that considers ion-ion, ion-electron and ion-neutral collisions will be computed in the near future using the XGC0 code [4].

Recent experiments were performed on NSTX to test the predicted variation of  $P_{LH}$  with  $R_x$  derived from X-transport theory. The two plasma shapes used in this study are shown in Figure 1a. The shapes have similar X-point height, plasma surface area, and outboard divertor poloidal length. The discharges ( $I_p = 800$  kA,  $B_T = 0.55$  T) were formed under three different fueling and pumping scenarios: (1) strong divertor pumping via lithium deposition and large neutral gas fueling, (2) weak divertor pumping (no inter-shot lithium deposition) and medium neutral gas fueling and (3) weak divertor pumping and low neutral gas fueling.

In each fueling scenario, the small- $R_X$  shape required more neutral beam heating power to achieve H-mode. For example, the weak pumping, medium fueling scenario required 2.6 MW of heating to achieve H-mode for the small- $R_X$  shape, while only 2.0 MW of heating is needed for the large- $R_X$  shape. This translates into a larger  $P_{LH}$  ( $= P_{heat} + P_{OH} - dW/dt$ ) for the small- $R_X$  shape (Fig 2a). These calculations assume 85% NBI heating efficiency and that fast ion contributions to the stored energy are minimal as guided by TRANSP calculations of similar L-mode discharges.

It is expected that the small- $R_X$  discharges will have larger edge  $T_i$  compared to the large- $R_X$  discharges since the core heating power is greater. However, it is difficult to use the traditional charge-exchange spectroscopy to measure the edge  $T_i$  and  $n_i$  in these discharges. This is due to the poor carbon confinement in L-mode and reduced neutral beam current injection required for this experiment. Thus, the electron temperature ( $T_e$ ) and density ( $n_e$ ) data measured by a multi-point Thomson scattering system are presented with the argument that  $T_i \sim T_e$  and  $n_i$  is proportional to  $n_e$  in the L-mode edge.

The midplane electron temperature and density profiles are fit with modified tanh functions. These fit profiles are used to compute  $\nabla(T_e n_e)/n_e$  ( $\sim \nabla(T_i n_i)/n_i$ ) which has a local minimum typically near  $\psi_N \sim 0.96$ . This expression is chosen since  $E_r \sim \nabla P_i / Z_i n_i$  in the plasma edge. Figure 2b and 2c show  $n_e$  and  $T_e$  respectively in the pedestal region at the local minimum. The edge  $n_e$  for each discharge pair of a fueling scenario is fairly well matched, while the edge  $T_e$  is 1.3 – 1.5 times larger in the small- $R_X$  case versus the large- $R_X$  case. Despite the large range in neutral beam heating in this database (0.3 – 2.6 MW) and

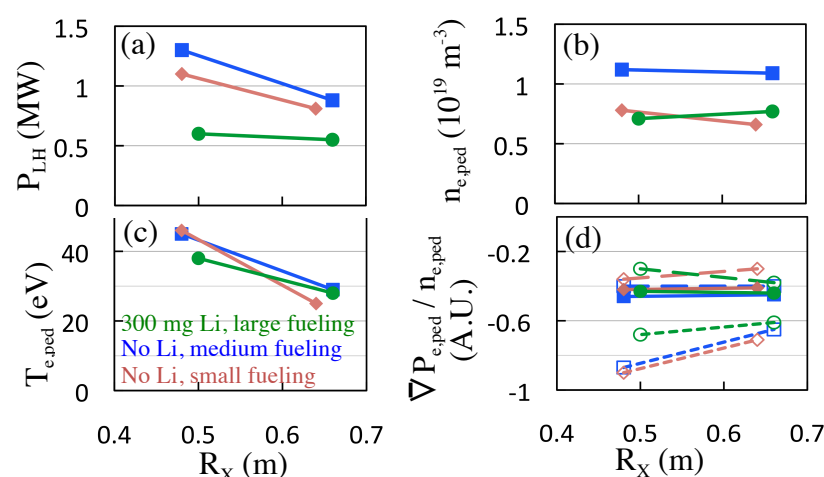


FIG 3 For  $R_X \sim 0.47$  m and  $R_X \sim 0.64$  shapes under three different fueling - pumping scenarios: (a)  $P_{LH}$ , (b)  $n_{e,ped}$ , (c)  $T_{e,ped}$  and (d) normalized  $\nabla P_e / n_e$  for two time points before LH transition and one after. The pedestal values in (b) - (d) are taken at the spatial location where  $\nabla P_e / n_e$  is a minimum.

thus very different core  $T_i$  and  $T_e$ , the edge  $T_e$  just prior to the LH transition is similar for discharges with the same shape.

The evolution of the local minimum in  $\nabla(T_e n_e)/n_e$  is shown in Figure 2d. The minimum value is plotted for the two L-mode profiles measured just prior to the

L-H transition and the first H-mode profile following the transition (each profile measurement is separated by 17ms). The empty symbols with long dashes and the solid symbols with solid lines are the L-mode measurements. The minimum becomes slightly more negative for each discharge as time advances. For the last measurement prior to the LH transition (solid lines), the normalized  $\nabla(T_e n_e)/n_e$  is about -0.4 for all discharges, regardless of the shape and fueling scenario. Following the LH transition, the minimum point becomes significantly more negative (open symbols, small dashes).

These results are consistent with the prediction that the small- $R_x$  shape requires about 60% higher edge ion temperatures to match the number of ion loss orbits in the plasma edge. The edge  $T_e$  prior to the L-H transition was  $\sim 42$  eV for the small- $R_x$  shape versus 28 eV for the large- $R_x$  shape. For all discharges in this database, which cover a wide range of neutral beam heating,  $R_x$  and fueling and pumping scenarios, the  $E_r$  profile estimate from the electron profiles are very similar just prior to the L-H transition. This is consistent with the hypothesis that the L-H transition is triggered near a critical  $E_r \times B$  mean flow or flow shear.

The edge  $T_e$  just prior to the L-H transition appears fairly independent of fueling and pumping scenario, neutral beam heating power and edge  $n_e$  for each shape considered. This reflects the variations of the coupling between the core heating and edge temperatures with plasma density, neutral fueling and divertor pumping.

The X-transport theory also predicts that most ions lost from the plasma edge will escape through the inner (outer) divertor leg in the favorable (un-favorable)  $\nabla B$  geometry. This leads to an electric potential between the divertor legs in L-mode that is proportional to the ion loss rate. The ion loss rate, and thus the electric potential, will quickly drop to near zero following the L-H transition. A potential consistent with the predictions of the X-transport model is routinely measured on NSTX discharges.

*This work was funded by the US Department of Energy under Contract Numbers DE-AC02-09CH11466 and DE-AC05-00OR22725. D.J. Battaglia is supported under an appointment to the U.S. DOE Fusion Energy Postdoctoral Research Program administered by ORISE under contract number DE-AC05-06OR23100 between the U.S. DOE and ORAU. Prepared by LLNL under Contract DE-AC52-07NA27344.*

<sup>1</sup> R. Maingi, et al., Nucl. Fusion (2010) 064010

<sup>2</sup> C.S. Chang, S. Ku, H. Weitzner, Phys. Plasmas, vol. 9, no. 9, (2002) 3884

<sup>3</sup> S. Ku, H. Baek, C.S. Chang, Phys. Plasmas, vol. 11, no. 12, (2004) 5626

<sup>4</sup> C.S. Chang, S. Ku, Contrib. Plasma Phys. 46, No. 7-9 (2006) 496